Proceedings of 2010 IEEE International Conference on Ultra-Wideband (ICUWB2010)

Enhanced-Accuracy Channel Estimation and Ranging for IR-UWB Energy Detectors

Bernhard C. Geiger*, Thomas Gigl*‡, and Klaus Witrisal*
*Signal Processing and Speech Communication Laboratory, Graz University of Technology, Austria
‡CISC Semiconductor, Design and Consulting GmbH, Austria
{geiger,thomas.gigl,witrisal}@tugraz.at

***Abstract*—The high temporal resolution of impulse radio ultra wideband (IR-UWB) communication systems makes these systems capable of obtaining high accuracies in ranging and channel estimation. At the same time, the required sampling rates and the associated complexity often prohibit the use of conventional digital (coherent) receivers. The energy detector, a non-coherent receiver, employs low sampling rates but suffers from reduced performance.**

In this work, the idea of multiple pulse transmissions is exploited to obtain highly accurate channel and range estimates using the low-complexity energy detector. A frequency offset is introduced between the sampling clock and the pulse repetition frequency. It is shown that with proper post-processing the quality of the channel estimate can be significantly increased and that time-of-arrival estimation accuracies in the order of 0.3 ns can be achieved independently of the integration period, using a 500 MHz UWB signal.

An appropriate receiver architecture is derived based on generic and IEEE 802.15.4a specific transmission parameters.

I. Introduction

Applications like positioning [1] and UWB radar [2] require an accurate estimation of the characteristics of the channel impulse response. While the necessary temporal resolution can be provided by using IR-UWB systems (pulse durations in the order of one nanosecond), a coherent receiver often has a prohibitively high complexity due to high sampling rates and extensive processing [3]. A non-coherent energy detector (ED) receiver is a low-complexity alternative, which recently gained momentum in the field of research [4].

While ranging with EDs has been studied extensively in the literature (e.g. [5], [6]), channel estimation so far is either relying upon coherent reception [7], [8] or requires computationally demanding post-processing [9]. In terms of ranging, [10] showed that the optimal receiver architecture in the generalized maximum likelihood sense slides an integration window of almost arbitrary duration over the received channel response. This sliding can be implemented either by a set of parallel EDs, or by a certain number of pulse repetitions and perfectly timed integration windows. In this work, a single ED is employed for channel estimation and ranging whose sampling rate is shifted with respect to the pulse repetition frequency. It is demonstrated that the signal model of the IEEE 802.15.4a standard [11] allows the application of the proposed receiver architecture.

Section II establishes a signal model, which is exploited for power delay profile (PDP) estimation in Section III. The possibility to refine the PDP estimate by means of equalization is introduced in Section IV. In Section V it is shown that the requirements imposed by the proposed receiver architecture are met by the signal model of the IEEE 802.15.4a standard, which is used for performance simulations in Section VI.

II. Signal Model

An equivalent baseband model of the system is used. Let the transmitted signal $s(t)$ be a train of M pulses $\phi(t)$

$$s(t) = \sqrt{E_{p,t}} \sum_{k=0}^{M-1} \phi(t - kT_{per}) \tag{1}$$

where $E_{p,t}$ is the transmitted pulse energy and T_{per} is the pulse repetition period. In this equation, $\phi(t)$ is a pulse with unit energy and a bandwidth W greater than 500 MHz. This signal is then transmitted over a multipath channel with impulse response

$$h(t) = \sum_{l=0}^{\infty} \alpha_l \delta(t - \tau_l) \tag{2}$$

where α_l and τ_l are the complex path gain and the path delay of the l-th multipath component (MPC), $\delta(t)$ is the Dirac delta function, and the time-of-arrival (TOA) is given by τ_0. The received signal is obtained by convolving $s(t)$ with the channel impulse response (CIR) $h(t)$:

$$\begin{aligned} r(t) &= \sqrt{E_{p,t}} \sum_{k=0}^{M-1} \sum_{l=0}^{\infty} \alpha_l \phi(t - kT_{per} - \tau_l) \\ &= \sqrt{E_{p,r}} \sum_{k=0}^{M-1} \phi_{mp}(t - kT_{per}) \end{aligned} \tag{3}$$

where $\phi_{mp}(t)$ is the channel response to the pulse shape $\phi(t)$ and $E_{p,r} = E_{p,t} \int_{-\infty}^{\infty} |\sum_{l=0}^{\infty} \alpha_l \phi(t - \tau_l)|^2 dt$ is the received pulse energy. For the proposed system architecture it is assumed that the pulse repetition period is larger than the maximum excess delay of the channel, i.e. $T_{per} \gg \tau_{\max}$, so that the responses from different pulses do not overlap.

III. System Model

Fig. 1 shows the ED, where the received signal $r(t)$ is first filtered with a filter $\phi^*(-t)$ matched to the pulse shape,

978-1-4244-5306-1/10/$26.00 ©2010 IEEE

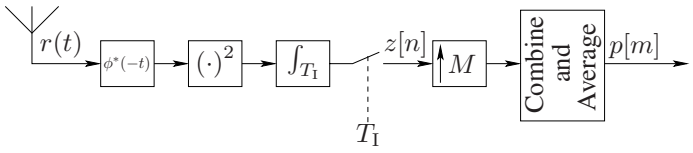

Fig. 1. Proposed Energy Detection Architecture for Channel Estimation

squared, integrated and periodically sampled at period T_I. The output $z[n]$ of the ED can thus be constructed as:

$$z[n] = \int_{(n-1)T_\mathrm{I}}^{nT_\mathrm{I}} |(r(t)+\eta(t)) * \phi^*(-t)|^2 dt$$
$$= \int_{(n-1)T_\mathrm{I}}^{nT_\mathrm{I}} \left| \sqrt{E_{p,r}} \sum_{k=0}^{M-1} g(t-kT_{per}) + \tilde{\eta}(t) \right|^2 dt \quad (4)$$

where $*$ is the convolution, $g(t) = \phi(t) * h(t) * \phi^*(-t)$ is the channel response to the filtered pulse, $\eta(t)$ is zero-mean complex Gaussian noise with a two-sided noise power spectral density (PSD) $\frac{N_0}{2}$, and $\tilde{\eta}(t)$ is the filtered version thereof.

A. Noise-Free System Model

Considering the noise-free case first, we have $\tilde{\eta}(t) = 0$ and due to the non-overlapping pulses we can write

$$z[n] = E_{p,r} \sum_{k=0}^{M-1} \int_{(n-1)T_\mathrm{I}}^{nT_\mathrm{I}} q(t-kT_{per}) dt \quad (5)$$

with $q(t) = |g(t)|^2$ being the instantaneous PDP of the channel. In order to ensure that for each of the M pulses the integration start instant of a continuously integrating ED is shifted relative to the pulse position, the integration period T_I must be a non-integer fraction of the pulse repetition period T_{per}. Setting T_I so that $NT_\mathrm{I} = T_{per} + T_s$ with $N \in \mathbb{N}$ leads to a shift of T_s relative to the pulse repetition period T_{per}, and we get

$$z[n] = E_{p,r} \sum_{k=0}^{M-1} \int_{(n-1)T_\mathrm{I}}^{nT_\mathrm{I}} q(t-kNT_\mathrm{I}+kT_s) dt. \quad (6)$$

After M symbols, the sum of all relative shifts T_s needs to cover one integration period T_I. Therefore we require $T_\mathrm{I} = MT_s$, and substituting the integration variable yields:

$$z[n] = E_{p,r} \sum_{k=0}^{M-1} \int_{(nM-kMN+k)T_s - T_\mathrm{I}}^{(nM-kMN+k)T_s} q(t) dt \quad (7)$$

for $n = 0, ..., MN-2$. From the sum of integrals only those are non-zero, for which k satisfies

$$0 < (nM - k(MN-1)) \leq \frac{T_{per}}{T_s} = MN - 1 \quad (8)$$

$$0 > k - n\frac{M}{MN-1} \geq -1. \quad (9)$$

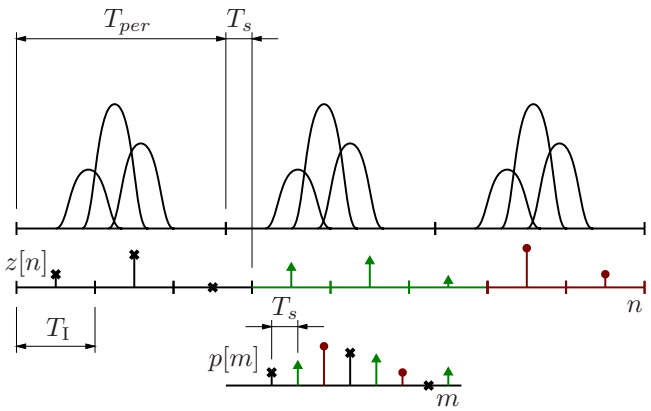

Fig. 2. Combining the ED output $z[n]$ to obtain a high-rate PDP estimate $p[m]$ (shown for the case $M = 3$)

This limits k to $\frac{nM - <nM>_{MN-1}}{MN-1}$, where $<\cdot>_L$ is the modulo-L operator. Using this in (7) it can be shown that

$$z[n] = E_{p,r} \int_{<nM>_{MN-1}T_s - T_\mathrm{I}}^{<nM>_{MN-1}T_s} q(t) dt. \quad (10)$$

The upsampled PDP estimate can be obtained by rearranging this sequence as shown in Fig. 2, i.e. $p[m] = \frac{1}{T_\mathrm{I}} z[<mN>_{MN-1}]$,

$$p[m] = \frac{E_{p,r}}{T_\mathrm{I}} \int_{<mMN>_{MN-1}T_s - T_\mathrm{I}}^{<mMN>_{MN-1}T_s} q(t) dt \quad (11)$$
$$= \frac{E_{p,r}}{T_\mathrm{I}} \int_{mT_s - T_\mathrm{I}}^{mT_s} q(t) dt = \frac{E_{p,r}}{T_\mathrm{I}} \sum_{n=-M+1}^{0} \int_{(m+n-1)T_s}^{(m+n)T_s} q(t) dt,$$

where the integral was split into M integrals. Assuming that T_s is sufficiently small, $\int_{(n-1)T_s}^{nT_s} q(t) dt \approx T_s q(nT_s)$ holds and we get with $q[n] = q(nT_s)$:

$$p[m] = \frac{E_{p,r}}{M} \sum_{j=-M+1}^{0} q[m+j] = E_{p,r} \left(q * h_\mathrm{MA}\right)[m] \quad (12)$$

where $h_\mathrm{MA}[n]$ is the impulse response of an M-th order moving average (MA) filter. According to this signal model, using $T_\mathrm{I} = MT_s = MNT_\mathrm{I} - MT_{per}$ the design equation for the receiver is

$$T_\mathrm{I} = \frac{MT_{per}}{MN-1} \quad (13)$$

with $N, M \in \mathbb{N}$.

B. Noise Performance Considerations

Introducing noise to the system, we have to go back to

$$z[n] = \int_{(n-1)T_\mathrm{I}}^{nT_\mathrm{I}} \left| \sqrt{E_{p,r}} \sum_{k=0}^{M-1} g(t-kT_{per}) + \tilde{\eta}(t) \right|^2 dt \quad (14)$$
$$= \int_{(n-1)T_\mathrm{I}}^{nT_\mathrm{I}} \sum_{k=0}^{M-1} \Big[E_{p,r} q(t-kT_{per}) + \nu_k(t) \Big] + |\tilde{\eta}(t)|^2 dt$$

where $\nu_k(t) = 2\sqrt{E_{p,r}}\Re\{g^*(t-kT_{per})\tilde{\eta}(t)\}$ is a zero-mean linear signal-by-noise crossterm, which is only non-zero within the support of $g(t-kT_{per})$. The integral over the quadratic noise term $|\tilde{\eta}(t)|^2$ follows a Γ-distribution with parameters [12], [13]

$$\int_{(n-1)T_\mathrm{I}}^{nT_\mathrm{I}} |\tilde{\eta}(t)|^2 dt \sim \Gamma\left(WT_\mathrm{I}, N_0\right). \tag{15}$$

Samples resulting from the linear and the quadratic noise term are also upsampled with factor M and rearranged according to Fig. 2. By transmitting an integer multiple N_{pr} of M pulses it is possible to average over N_{pr} pulse trains and improve performance by reducing the noise variance[1]. Moreover, the influence of the linear noise term $\nu_k(t)$ vanishes with increasing N_{pr} [14].

For sufficiently large N_{pr} the Γ-distribution can be approximated by a Gaussian distribution and the noise-only portion of the PDP estimate $p[m]$ follows

$$\Gamma\left(WN_{pr}T_\mathrm{I}, \frac{N_0}{N_{pr}T_\mathrm{I}}\right) \approx \mathcal{N}\left(WN_0, \frac{WN_0^2}{N_{pr}MT_s}\right). \tag{16}$$

From this it can be shown, that for a given received pulse energy $E_{p,r}$ and a given resolution T_s the robustness increases with $\sqrt{M}$: The standard deviation of the noise samples decreases with $\sqrt{M}$ while the signal energy is independent of M (see (12)). If, on the other hand, the energy of the pulse train $E_{t,r} = ME_{p,r}$ is constrained, $E_{p,r}$ in (12) reduces with M and, consequently, robustness decreases with $\sqrt{M}$.

C. Filtering

It is important to note that due to the receiver architecture consecutive noise samples are independent. The sampling rate of the PDP estimate is T_s but the deterministic part of the signal is confined to a bandwidth $W < \frac{1}{T_s}$ (effectively even less due to MA filtering). Therefore it is possible to apply a filter with bandwidth W to reduce the variance of the noise portion by a factor of WT_s.

IV. Equalization

In Section III it was shown that the obtained PDP estimate $p[m]$ can be modeled as a noisy version of the MA filtered PDP $q[m]$, or mathematically

$$p[m] = E_{p,r}\left(q * h_\mathrm{MA}\right)[m] + n[m] \tag{17}$$

where $n[m]$ accounts for both the linear and the quadratic noise term. It is assumed that $n[m]$ is Gaussian and zero-mean, which holds for sufficiently high N_{pr} to average over and after stripping off the mean value. In vector notation this yields

$$\mathbf{p} = E_{p,r}\mathbf{H}_\mathrm{MA}\mathbf{q} + \mathbf{n} \tag{18}$$

where $\mathbf{H}_\mathrm{MA}$ is the convolution matrix of the MA filter. The equalized PDP estimate $p_{eq}[m]$ is obtained by minimizing the mean square error (MSE), i.e.

$$\mathbf{p}_{eq} = \arg\min_{\mathbf{q}} \left\{||\mathbf{p} - E_{p,r}\mathbf{H}_\mathrm{MA}\mathbf{q}||^2\right\} \tag{19}$$

$$= \left(\frac{\sigma_n^2}{\sigma_q^2}\mathbf{I} + E_{p,r}^2\mathbf{H}_\mathrm{MA}\mathbf{H}_\mathrm{MA}^T\right)^{-1} E_{p,r}\mathbf{H}_\mathrm{MA}\mathbf{p} \tag{20}$$

with $\sigma_n^2 = \mathrm{Var}\{n[m]\}$ and σ_q^2 is the variance of the signal[2]. Since it is often not desired to continuously estimate the noise variance and since the variance of the signal not only depends on the received energy $E_{p,r}$ but also on the channel characteristics, $\frac{\sigma_n^2}{\sigma_q^2}$ will be treated as a design parameter for the equalizer. Another design parameter implicit in the dimensionality of the convolution matrix $\mathbf{H}_\mathrm{MA}$ is the order of the equalizer filter.

Knowing that the MA filter acts as a low-pass, its equalizer can be assumed to amplify higher frequencies stronger than lower ones. Since frequencies above $\frac{W}{2}$ contain only noise, equalization suffers from poor robustness. By filtering according to Section III-C, the obtained PDP estimate $p_{f,eq}[m]$ becomes less susceptible to noise.

V. Channel Estimation in the IEEE 802.15.4a

It is shown next that the design equation (13) can be fulfilled by the signal model of the IEEE 802.15.4a standard [11]. According to this standard, every transmission is preceded by a preamble for synchronization and ranging, which consists of a certain number $N_{sync} \in \{16, 64, 1024, 4096\}$ of symbol repetitions. The symbols are generated by modulating pulses with a code sequence of length $N_{code} \in \{31, 127\}$ consisting of ternary elements $\{-1, 0, 1\}$. The time between consecutive pulses is LT_C, where $T_C \approx 2$ ns is the chip duration and $L \in \{4, 16, 64\}$ is the spreading factor. Since the number of non-zero code elements is $N_N = \frac{N_{code}+1}{2}$, the transmit energy of a preamble symbol is equal to $E_{p,t} = N_N E_p$ with E_p being the pulse energy. The symbol duration of a preamble symbol can be calculated as $T_{sym} = N_{code}LT_C$.

The most remarkable feature of the IEEE 802.15.4a standard is that the defined code sequences share perfect circular correlation properties with the transmitted code sequence after coherent or non-coherent reception [15]. In other words, after correlation at the receiver, all N_N pulses in the preamble symbol are combined to a single pulse with energy $E_{p,r} = N_N E_p \int_{-\infty}^{\infty} |\sum_{l=0}^{\infty} \alpha_l \phi(t-\tau_l)|^2 dt$ if the responses from consecutive pulses do not overlap (i.e. $LT_C > \tau_\mathrm{max}$) [14]. As a consequence, the received preamble can be modeled as a train of N_{sync} pulses with a pulse repetition period $T_{per} = T_{sym}$. If furthermore $N_{sync} \geq N_{pr}M$ the signal model from Section II applies and high-resolution channel estimation can be performed. Since correlation is performed after upsampling, the local code sequence has to be upsampled to T_s as well. To keep the correlation process simple, T_s is constrained to

[1] Unfortunately, due to non-coherent combination only a fraction of this additional energy can be exploited [3].

[2] Note that the zero-forcing equalizer yields an unstable solution since the MA filter has M zeros on the unit circle.

TABLE I
A SET OF POSSIBLE RECEIVER PARAMETERS IN AN IEEE 802.15.4A FRAMEWORK ($N_{code} = 31$, $L = 16$, $T_{per} = 992$ ns)

T_I ns	M -	T_s ns	N -	$N_{pr}M$ (N_{pr}) $N_{sync} = 16$	$N_{pr}M$ (N_{pr}) $N_{sync} = 64$
1.75	7	0.25	567	14 (2)	63 (9)
2.25	9	0.25	441	9 (1)	63 (7)
2.5	5	0.5	397	15 (3)	60 (12)
2.75	11	0.25	361	11 (1)	55 (5)
3	3	1	331	15 (5)	63 (21)
3.75	15	0.25	265	15 (1)	60 (4)
4.25	17	0.25	234	– (0)	51 (3)
5	5	1	199	15 (3)	60 (12)

be an integer fraction of T_C. Unfortunately, according to the standard N_{sync} is restricted to certain values, which makes it impossible to exploit the full preamble energy. Table I shows possible choices of T_I and the resulting number of exploitable symbols $N_{pr}M$. It can be seen that with increasing N_{sync} a smaller fraction of the preamble energy is lost. It is more important, however, that shorter integration periods T_I allow for averaging over a larger number of pulse trains N_{pr}, which according to (16) leads to a reduction of noise effects.

Another benefit of the IEEE 802.15.4a signal model is that the requirement on N_{pr} is loosened concerning the validity of the Gaussian approximation in noise performance derivation in (16): Since correlation can be interpreted as a weighted summation of N_{code} noise samples, the correlation process already justifies (16) without requiring N_{pr} to be large. Moreover, as [16] shows, it is possible to design a zero-mean code sequence so that in the correlation process the mean value is automatically stripped.

VI. Simulations and Results

To compare the different proposed receiver architectures against each other in terms of robustness, ranging, and channel estimation accuracy, a series of simulations was performed. The signal model used in these simulations follows the IEEE 802.15.4a standard [11], where the pulse shape $\phi(t)$ is a root raised-cosine filtered pulse with a duration of $T_p = 2$ ns and a roll-off factor $\beta = 0.6$, thus $W = \frac{1}{T_p} = 500$ MHz. The short codes with $N_{code} = 31$ and a spreading factor $L = 16$ were chosen. For sake of simplicity and regardless of the definitions of the standard, the number of symbol repetitions N_{sync} was set to M unless otherwise noted. To obtain a sufficient resolution for channel estimation, T_s was set to 0.25 ns, while T_I was varied within $\{1.75, 2.25, 3.75, 4.25\}$ ns. The corresponding values for M can be seen in Table I.

The channel model was adopted from [17], which is an exponentially decaying model where the arrival times of the MPCs τ_l are derived from a Poisson process. For the simulations, the Poisson arrival rate was set to 5 MPCs per ns, the Ricean K-factor was set to 1 to account for a line-of-sight scenario and the RMS delay spread was set to $\tau_\mathrm{RMS} = 5$ ns. This setting guarantees that the CIR is short enough so that the responses from subsequent pulses do not overlap. For each integration period and each receiver architecture a set of $N_{sim} = 1000$ channels was simulated.

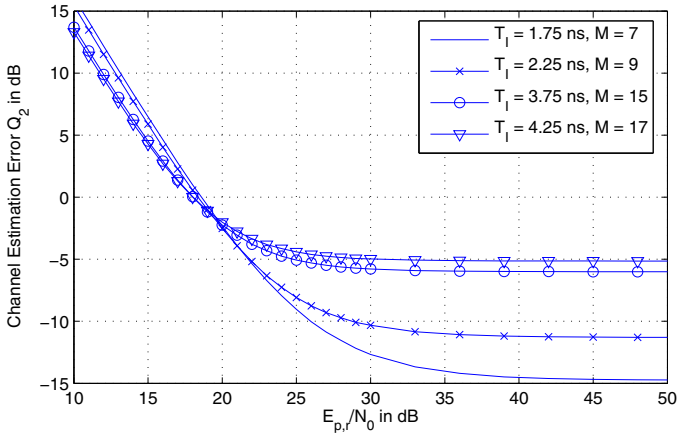

Fig. 3. Channel estimation error of the PDP estimate $p[m]$ for different values of T_I.

Filtering for noise reduction after combining symbols was implemented using an ideal low-pass filter with bandwidth W. Equalization was performed with a 40^{th}-order filter, and the design parameter $\frac{\sigma_n^2}{\sigma_q^2}$ was set to 0.001, which yields highly accurate PDP estimates $p_{eq}[m]$ and $p_{f,eq}[m]$ [13].

The quality of the estimates was obtained by computing the channel estimation error

$$Q_2 = \frac{1}{N_{sim}} \sum_{i=1}^{N_{sim}} \frac{\sum_m \left(p^{(i)}[m] - q^{(i)}[m]\right)^2}{\sum_m q^{(i)}[m]^2} \qquad (21)$$

where the superscript (i) indicates the i-th channel realization and where $p[m]$ can be exchanged by $p_f[m]$, $p_{eq}[m]$, or $p_{f,eq}[m]$, depending if the receiver employs noise reduction by filtering, equalization, or both.

Ranging was implemented as TOA estimation via threshold comparison confined to a search-back window preceding the maximum sample of the PDP estimate (MES-SB, introduced in [6]). The size of the search-back window was set to 32 ns and the optimum threshold was chosen for each value of $\frac{E_{p,r}}{N_0}$. The ranging accuracy is denoted by the mean absolute error (MAE), which is defined as

$$\mathrm{MAE} = \frac{1}{N_{sim}} \sum_{i=1}^{N_{sim}} |\tau_0 - \hat{\tau_0}^{(i)}|. \qquad (22)$$

TOA estimates $\hat{\tau_0}^{(i)}$ obtained from the PDP estimates were compared against a receiver architecture performing ranging directly on the output $z[n]$ of the ED. This latter structure exploits all M symbols for averaging [16].

A. Channel Estimation

Fig. 3 shows the quality of the unfiltered, unequalized PDP estimate $p[m]$ for different values of the integration period T_I. It can be seen that in terms of SNR robustness, larger integration periods (and, consequently, larger values of M) outperform smaller values of T_I. This is in accordance with Section III-B, where the standard deviation of the noise-only portion was shown to decrease with $\sqrt{M}$ compared to the

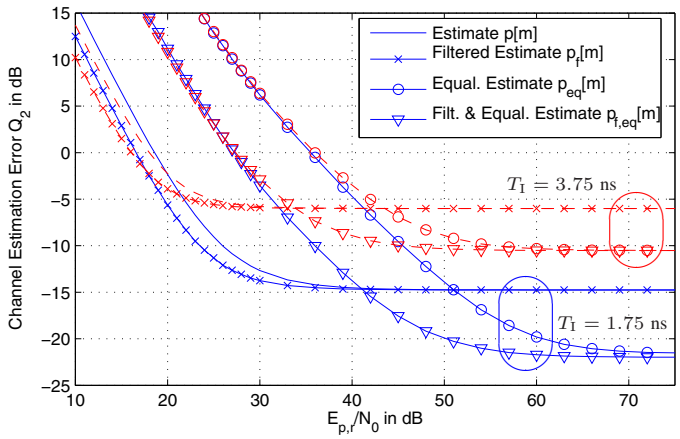

Fig. 4. Comparison between the channel estimation error of different receiver architectures. The integration period was set to $T_\mathrm{I} = 1.75$ ns ($M = 7$, solid) and $T_\mathrm{I} = 3.75$ ns ($M = 15$, dashed)

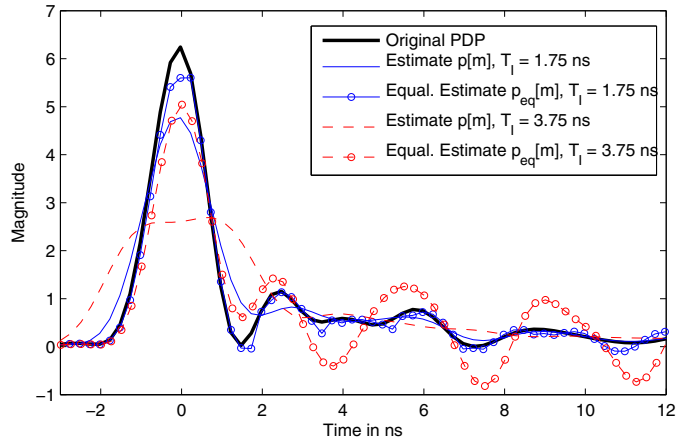

Fig. 5. Channel estimation with and without equalization for $T_\mathrm{I} = 1.75$ ns ($M = 7$) and $T_\mathrm{I} = 3.75$ ns ($M = 15$). $\frac{E_{p,r}}{N_0}$ was set to 50 dB.

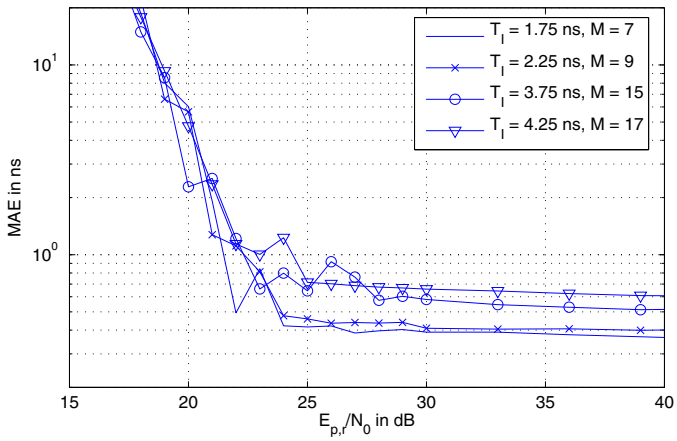

Fig. 6. Ranging error of the PDP estimate $p[m]$ for different values of T_I.

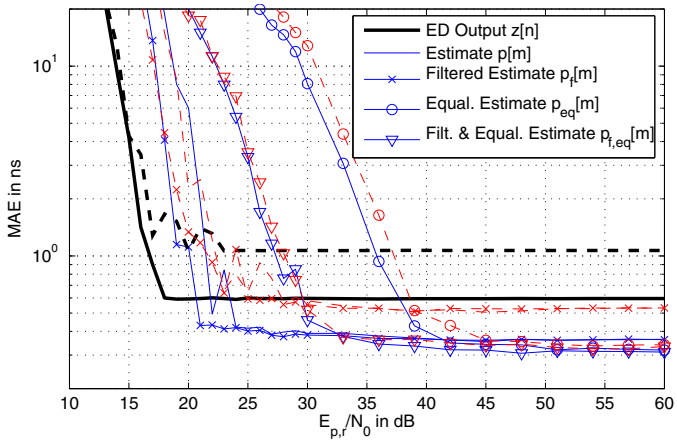

Fig. 7. Comparison of the ranging error for different receiver architectures. The integration period was set to $T_\mathrm{I} = 1.75$ ns ($M = 7$, solid) and $T_\mathrm{I} = 3.75$ ns ($M = 15$, dashed) for channel estimation architectures and to $T_\mathrm{I} = 2$ ns (solid, bold) and $T_\mathrm{I} = 4$ ns (dashed, bold) for the direct architecture.

received symbol energy $E_{p,r}$. This robustness comes at the cost of an M times increased pulse train energy. Moreover, it can be seen that a higher order M of the MA filter leads to decreased channel estimation performance in regions where the SNR is high.

A comparison between different receiver architectures can be seen in Fig. 4, which shows that filtering indeed increases robustness and that this increase is bigger if an equalizer is used. For high SNR, the curves for the PDP estimates with and without filtering fall together, which is intuitively understood. As Fig. 4 shows, equalization yields a big increase in channel estimation accuracy, but this increase comes at the cost of reduced robustness. The high noise gain obviously prevents the equalizer from working properly at low to medium SNR.

Unfortunately, equalization cannot overcome the decrease in channel estimation accuracy for increasing T_I. This can be explained by looking at Fig. 5, which shows the channel estimates $p[m]$ and $p_{eq}[m]$ for $T_\mathrm{I} = 1.75$ ns and $T_\mathrm{I} = 3.75$ ns. It can be seen that the equalizer manages to recover the first few MPCs, whereas it tends to oscillate at the tail of the CIR. These oscillations are more severe for larger MA filter orders M (or, equivalently, for larger T_I), which explains why in Fig. 4 the accuracies of the equalized PDP estimates for different T_I do not meet. Indeed it can be seen that the improvement by equalization is smaller for larger T_I, corresponding to this reasoning.

B. Ranging

In Fig. 6 the performance of MES-SB applied to the PDP estimate $p[m]$ is shown for different values of T_I. Again, it can be seen that larger integration periods lead to decreased ranging accuracy, which can be related to the fact that due to MA filtering high-frequency components of the PDP cannot be resolved. The comparison between different architectures can be seen in Fig. 7. In accordance with the discussion in Section VI-A, robustness can be improved by filtering but suffers from equalization. Here, however, an interesting fact can be observed: Equalization manages to reverse the effects of MA filtering and obtains a ranging accuracy independent

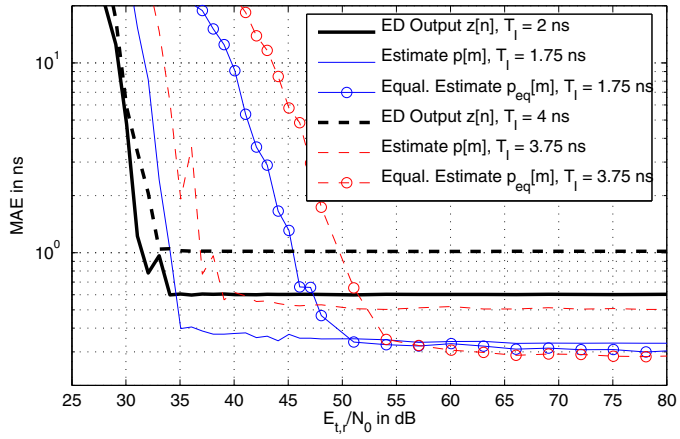

Fig. 8. Comparison between the ranging error of different receiver architectures in an IEEE 802.15.4a framework.

of T_I, albeit with increased SNR requirements. Confering to Fig. 5, the reader can see that the first few MPCs – which are of vital importance for ranging – are almost completely recovered. This fact opens the way to low-complexity ED receiver architectures capable of achieving highly accurate range estimates.

Ranging performed directly on the output of the energy detector exploits all M symbols for noise averaging and thus has a higher robustness. Since according to [6] the minimum MAE for this method is $\frac{T_\mathrm{I}}{4}$, accuracy is comparably poor (see Fig. 7). For the proposed architecture on the other hand, the minimum MAE reduces to $\frac{T_s}{4}$ independently of T_I.

C. Performance in the IEEE 802.15.4a Standard

A final set of simulations investigates the performance of the proposed receiver architectures in an IEEE 802.15.4a framework, where instead of the symbol energy $E_{p,r}$ the preamble energy $E_{t,r}$ was fixed. For these simulations the number of symbol repetitions in the preamble was set to $N_{sync} = 64$, which is in full accordance with the standard [11]. Thus, the energy of the whole preamble is $E_{t,r} = N_{sync} E_{p,r}$.

According to Table I, for an integration period of $T_\mathrm{I} = 1.75$ ns the receiver can average over $N_{pr} = 9$ pulse trains, while for $T_\mathrm{I} = 3.75$ ns this value is reduced to $N_{pr} = 4$. As shown in Fig. 8, indeed the short integration period clearly outperforms the longer one in terms of robustness because of improved noise averaging. Given a fixed number of symbol repetitions, a trade-off between receiver complexity (in terms of T_I) and noise sensitivity has to be made.

VII. Conclusion

In this work a receiver architecture for channel estimation using an energy detector is proposed. A high-rate estimate is obtained by repeatedly shifting the integration start instant relative to the pulse position. It is shown that this architecture poses minor requirements on the transmission schemes of the IR-UWB communication system, and that these requirements are met by devices compliant to the IEEE 802.15.4a standard.

It is also shown that the channel estimates can be used for the purpose of ranging and that with proper equalization the accuracy can be made independent of the integration period. Although equalization suffers from reduced robustness, in regions of sufficiently high SNR a mean absolute error of 0.3 ns can be achieved for an integration interval of 3.75 ns. It turns out that the proposed architecture clearly outperforms other threshold-based ranging systems introduced in the literature.

References

[1] S. Gezici, Z. Tian, G. B. Giannakis, H. Kobayashi, A. F. Molisch, H. V. Poor, and Z. Sahinoglu, "Localization via ultra-wideband radios: a look at positioning aspects of future sensor networks," *IEEE Signal Processing Magazine*, vol. 22, no. 4, pp. 70–84, July 2005.

[2] J. D. Taylor, *Introduction to Ultra-Wideband Radar Systems*. CRC Press, 1994.

[3] T. Gigl, F. Troesch, J. Preishuber-Pfluegl, and K. Witrisal, "Maximal operating distance estimation for ranging in IEEE 802.15.4a ultra-wideband," in *IEEE Workshop on Positioning, Navigation, and Communication (WPNC)*, March 2010, in press.

[4] K. Witrisal, G. Leus, G. J. Janssen, M. Pausini, F. Troesch, T. Zasowski, and J. Romme, "Noncoherent ultra-wideband systems," *IEEE Signal Processing Magazine*, vol. 26, no. 4, pp. 48–66, July 2009.

[5] D. Dardari, A. Conti, U. Ferner, A. Giorgetti, and M. Z. Win, "Ranging with ultrawide bandwidth signals in multipath environments," *Proceedings of the IEEE*, vol. 97, no. 2, pp. 404–426, February 2009.

[6] I. Guvenc and Z. Sahinoglu, "Threshold-based TOA estimation for impulse radio UWB systems," in *IEEE Int. Conf. on Ultra-Wideband (ICU)*, September 2005, pp. 420–425.

[7] V. Lottici, A. D'Andrea, and U. Mengali, "Channel estimation for ultra-wideband communications," *IEEE Journal on Selected Areas in Communications*, vol. 20, no. 9, pp. 1638–1645, December 2002.

[8] I. Maravic, M. Vetterli, and K. Ramchandran, "Channel estimation and synchronization with sub-Nyquist sampling and application for ultra-wideband systems," in *IEEE Int. Sym. on Circuits and Systems (ISCAS)*, May 2004, pp. V381–V384.

[9] S. Mekki, J.-L. Danger, B. Miscopein, and J. J. Boutros, "EM channel estimation in a low-cost UWB receiver based on energy detection," in *IEEE Int. Sym. on Wireless Communication Systems (ISWCS)*, October 2008, pp. 214–218.

[10] A. Rabbachin, I. Oppermann, and B. Denis, "GML ToA estimation based on low complexity UWB energy detection," in *IEEE Int. Sym. on Personal, Indoor and Mobile Radio Communications (PIMRC)*, September 2006, pp. 1–5.

[11] IEEE Working Group 802.15.4a, "Wireless medium access control (MAC) and physical layer (PHY) specifications for low-rate wireless personal area networks (LR-WPANs)," IEEE, Tech. Rep., August 2007.

[12] H. Urkowitz, "Energy detecction of unknown deterministic signals," *Proceedings of the IEEE*, vol. 55, no. 4, pp. 523–531, April 1967.

[13] B. Geiger, "Enhanced accuracy channel estimation and ranging for energy detectors," Master's thesis, Signal Processing and Speech Communication Laboratory, Graz University of Technology, 2009.

[14] T. Gigl, J. Preishuber-Pfluegl, and K. Witrisal, "Statistical analysis of a UWB energy detector for ranging in IEEE 802.15.4a," in *IEEE Int. Conf. on Ultra Wideband (ICUWB)*, September 2009, pp. 129–134.

[15] Y.-S. Kwok, F. Chin, and X. Peng, "Ranging mechanism, preamble generation, and performance with IEEE 802.15.4a low-rate low-power UWB systems," in *IEEE Sym. on Spread Spectrum Techniques and Applications*, September 2006, pp. 525–530.

[16] B. Geiger, "Ranging in the IEEE 802.15.4a standard using energy detectors," in *IEEE EUROCON*, May 2009, pp. 1948–1955.

[17] K. Witrisal and M. Pausini, "Statistical analysis of UWB channel correlation functions," *IEEE Transactions on Vehicular Technology*, vol. 53, no. 3, pp. 1359–1373, March 2008.